Nuclear Engineering and Design 373 (2021) 110836

Contents lists available at ScienceDirect

Nuclear Engineering and Design

journal homepage: www.elsevier.com/locate/nucengdes

Multiphysics CATHARE2 modeling and experimental validation methodology against CABRI transients

J.-M. Labit [a], N. Marie [a,*], O. Clamens [a], E. Merle [b]

[a] CEA, DEN, DER, F-13108 Saint Paul-Lez-Durance, France
[b] CNRS-IN2P3-LPSC/Grenoble INP/UGA, 53 Rue des Martyrs, 38026 Grenoble Cedex, France

ARTICLE INFO

Keywords:
CABRI
Multiphysics
RIA
Validation
CATHARE

ABSTRACT

CABRI is an experimental pulse reactor, funded by the french Institute for Radiological protection and Nuclear Safety (IRSN) and operated by CEA at the Cadarache nuclear center, France. Its aim is to study and thus to better understand RIA (Reactivity-Initiated Accident) effects on nuclear fuels.

The restart of the CABRI reactor in 2015 offers the opportunity to validate tools involving multiphysic calculation schemes on reactivity insertions (RI) transients at a system scale. Physics of the in-pile CABRI tests is complex and implies various physical fields (solid and fluid thermics, thermal-hydraulics, mechanics and neutronics) and their coupled effects. The reactivity insertion in CABRI is mastered by the depressurization of a neutron absorber (^{3}He), contained into transient rods. The increase of the neutron flux inside the core induces the neutronic power increase inside the core and a multiphysic effect, called "TOP" effect, inside the in-core transient rods that causes an acceleration of the gas depressurization.

The challenge is thus to manage the simulation of these RIA complex transients catching the governing multiphysical phenomena to be identified. In order to achieve this objective, a model for the CABRI transients and a scientific calculation tool have been developed and should be validated. This paper proposes a modeling of governing multiphysic phenomena of RIA transients in CABRI reactor based on a Quantified Phenomena Identification and Ranking Table (QPIRT). These models are introduced in the CATHARE2 tool in a dedicated version named PALANTIR and Best-Estimate simulation results are compared with experimental data obtained on CABRI commission tests: core power and ^{3}He pressure evolution.

1. Introduction

Nowadays, the simulations of coupled multiphysic phenomena occurring in nuclear reactors quickly rise (Salah et al., 2003). This field of research is likely to continue and to further increase in the years to come thanks to the fast increase in software computing capacity. The advancements in numerical methods and computer technology together with the continuous increase in operational experience have been moved in the last few years towards the investigation of realistic (or Best-Estimate) simulations of coupled complex phenomena under accidental scenarios in nuclear power plants. Hence, several activities (even international program (Salah et al., 2003) have been completed or are in progress to demonstrate the capabilities of coupled methods (Pascal et al., 2020; D'Auria et al., 2004) and multiphysic simulation tools in performing, in a Best-Estimate way, such complex transients.

CABRI reactor is an experimental pulse pool-type research reactor, funded by IRSN and operated by CEA at the Cadarache nuclear center in France. It is designed to experimentally simulate a sudden power increase, typical of a Reactivity-Initiated Accident. This type of accident is considered in the safety analysis of PWRs. The CABRI experiments constitute a real opportunity to collect valuable data on such complex multiphysic transients.

The challenge is thus to succeed the simulation of the reactivity initiated transients performed in the CABRI reactor catching the governing multiphysic phenomena. The present work leans on the CATHARE2 tool to which new models have been added following a Quantified Phenomena Identification and Ranking Table (QPIRT).

In this paper, we firstly addressed the main features of the CABRI reactor and the multiphysic phenomena involved in the reactivity insertion (RI) transients to go until a classification of those phenomena. Then, the third section presents the new models implemented in CATHARE2. They concern the improvement of the neutronic point-kinetics method to handle 3D effects in the core, the coupled

* Corresponding author.
E-mail addresses: jean-marc.labit@cea.fr (J.-M. Labit), nathalie.marie@cea.fr (N. Marie).

https://doi.org/10.1016/j.nucengdes.2020.110836
Received 12 February 2020; Received in revised form 24 June 2020; Accepted 31 August 2020
Available online 21 October 2020

Nomenclature

Acronyms

(Q) PIRT	(Quantified) Phenomena Identification Ranking Table
BC	Boundary condition
CABRI	French experimental reactor dedicated to safety studies
CATHARE	Code for Analysis of THermalhydraulics during an Accident of Reactor and safety Evaluation
CEA	Commissariat à l'Energie Atomique et aux Energies Alternatives (French Alternative Energies and Atomic Energy Commission)
CSR	Control and Safety Rods
DNB	Departure from Nucleate Boiling
EDF	Electricité De France
FB	Feedback
FWHM	Full Width at Half-Maximum
IRSN	Institut de Radioprotection et de Sûreté nucléaire (Institute for Radiological protection and Nuclear Safety)
ONB	Onset of Nucleate Boiling
PALANTIR	in French "Projet d'Amélioration des Lois et Approximations en Neutronique et Thermohydraulique pour les Insertions de Réactivité " - Project of Advancements in Laws and Approximations in Neutronics and Thermal-hydraulics during Insertions of Reactivity
PWR	Pressurized Water Reactor
RI	Reactivity Insertion
RIA	Reactivity Initiated Accident
SD1, SD2	Single depressurization respectively via the high flowrate and low flowrate channel
TOP	Transient OverPower
TRIPOLI	Tridimensionnel Polycinétique: CEA's stochastic neutronic code
URANIE	CEA's uncertainty analysis platform
VABT03, VABT04	Control valves, respectively of the high flowrate and low flowrate channel

Geometry

h, c, e, r, h_{valve}	Core height (m), fuel rods pitch (m), thickness (m), radius (m), valve stem position (m)

Neutronics

A	Anti-reactivity coefficient
P_n	Neutronic power (W)
ρ	Reactivity
σ_{TOP}	Microscopic cross section of $^3He(n;p)^3H$ reaction (barn)
e_{TOP}	Energy released by a $^3He(n;p)^3H$ reaction (J)
F_z, F_{xy}	Axial and radial power profiles
Φ	Neutron flux (n/cm^2/s)
p_v	Volumic power generated into the fluid by a TOP reaction (W/m^3)

Subscripts

0	Initial
∞	Bulk
c	Clad
conv	Convection
ext, *int*	External, internal
ext, *mod*, *dop*, *dil*	For neutronic variables: external, moderator, Doppler and clad expansion
f	Fluid
l	Liquid
p	Pellet
sat	Saturation
tr, *st*	Transient, steady-state
v	Vapour

Thermal-hydraulics

α	Volumic void fraction when used without subscript
α_i	Thermal diffusion coefficient (m^2.s^{-1}) when used with subscripts
β	Thermal expansion coefficient (K^{-1})
λ	Conductivity (W.m^{-1}.K^{-1})
ρ	Density (kg.m^{-3})
τ	Characteristic time (s)
ξ	Head loss coefficient
Bi	Biot number
c_p	Heat capacity (J.kg^{-1}.K^{-1})
C_v	Valve capacity
E	Energy released in the fuel (J)
h	Heat exchange coefficient (W.m^{-2}.K^{-1}) used with subscripts
M_{He}	Helium molar mass (kg/mol)
N_A	Avogadro constant (mol^{-1})
N_t	Number of fuel rods
Nu	Nusselt number
Pr	Prandtl number
R	Ideal gas constant (J/mol/K)
Re	Reynolds number
T, P, v	Temperature (K), pressure (Pa), fluid velocity (m/s)
x_T	Maximal pressure drop ratio in the valve

modeling of the transient rods circuit with the reactor circuit and the depressurization of Helium in these transient rods that induces the reactivity insertion inside the core. This depressurization is subjected to the "TOP" effect (Clamens et al., 2018) which is also modeled. The thermomechanical model describing the evolution of the gap between the pellet and the clad and its associated heat exchange as well as the model of single phase transient heat exchanges between the clad and the fluid are presented. Finally, in Section 4, results of Best-Estimate simulations of various kinds of RI transients obtained with this improved CATHARE2 tool, called CATHARE2 PALANTIR, are compared to CABRI experimental transient results.

2. Context and RIA transients

2.1. CABRI reactor

CABRI is a water-cooled reactor able to reach 23.7 MW power level for steady state (Hudelot et al., 2016). Its core consists of 1487 UO_2 fuel rods (enrichment: 6%), reaching the initial conditions by means of 6 Control and Safety Rods in hafnium (Fig. 1). One of the main particularities of the reactor is its reactivity injection system which is used to perform the power transient. The RIA transients considered in safety demonstration postulate the ejection of a control rod as accident initiator. The very rapid increase in reactivity due to a potential control rod ejection is recreated inside the CABRI reactor by the depressurization of

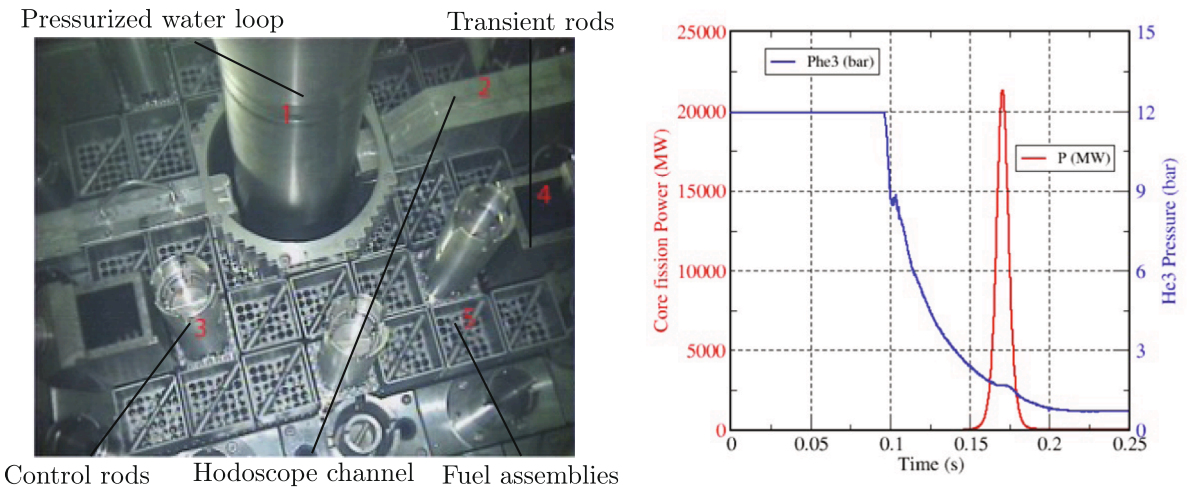

Fig. 1. A view of the CABRI core and an example of power pulse and depressurization of transients rods.

^{3}He from four "transient rods" located inside the core and connected to low and high flow rate channels towards a dump tank. These transient rods enable the realization of various types of transients. Depressurizations that are made through high flow rate channel are called "SD1" (simple depressurization 1), and the ones that are made through low flow rate channel are called "SD2".

Before the test, the transient rods are filled with ^{3}He, a neutron-absorbing gas. The power transient is generated with controlled opening of the fast valves so that the helium under pressure can escape. This results in a sudden increase in reactivity (since the neutrons are no more absorbed, the fission rate increases) and thus to a power peak (the pulse). This is immediately limited by neutron counter-reactions, mainly Doppler feedback effect, then at a lower level, clad expansion and moderating feedback effects. When the difference between initial insertion of reactivity (induced by helium depressurization) and anti-reactivity becomes lower than 1 $, the core power decreases. Finally, the core is completely shut down by the control rods drop. The pulses last from several milliseconds to several tens of milliseconds (characterized by a width at half-maximum between 7 and 93 ms (Clamens, October 2018), with instantaneous power up to 21 GW, and energy deposited in the core can that reach up to 250 MJ during a transient. The core is cooled with a forced convection water loop and the whole system is immersed in a pool.

An example of such a transient results is given in Fig. 1 by their ^{3}He pressure and power evolutions. The initial ^{3}He pressure and its kinetics of depressurization in the four transient rods circuit can lead to many kinds of power pulses, with various heights and widths at half-maximum. Transients are thus characterized by their maximum power, their Full Width at Half Maximum (FWHM) and energy deposit. Thus the short FWHM power transients will be generated by the opening of the unique high flow rate channel. The maximum power is then very high (10 to 20 GW) and the FWHM is short (~10 ms), due to the reactivity insertion dynamics. The energy deposit in this case depends on the initial pressure in the transient rods, the control valve aperture and the control rods drop time. In order to be representative of accidental power plant conditions, the FWHM of the transient is managed by opening successively the fast opening valves of the low flow rate and then the high flow rate channels (called "double depressurizations").

Various types of measurements are available for each test (Jeury et al., 2013; Lecerf et al., 2017):

- water temperatures in the primary cooling system, at the inlet and the outlet of the core;
- water flow rate in the primary cooling system at the inlet of the core;
- pressure of ^{3}He in transient circuit;
- neutronic power inside the core.

2.2. Calculation tools for CABRI transients simulation

Two calculation tools have been specially developed in order to simulate CABRI transients: DULCINEE (Ritter et al., 2012) and SPARTE (Clamens et al., 2018). DULCINEE was developed in the 1970s (Ritter et al., 2012 to design and characterize the behavior of the CABRI core during several types of transients (RIA, overpower…). DULCINEE embeds 0D and 1D simplified thermal and thermal-hydraulic models. The thermal-hydraulics can process steady single or double phase flows in forced convection. Several types of regions are described (fuel/gap/clad). With DULCINEE, the CABRI core is modeled with 2 regions: 1 hot channel and the remaining average channels. DULCINEE allows assessing the transient power from the knowledge of the external reactivity (reactivity injected by transient rods depressurization) as a function of time and point kinetics equation with neutronic parameters given by TRIPOLI4 (Brun et al., 2011) using the JEFF3.1.1 nuclear database and the iterated fission probability method. SPARTE has been developed in order to improve the DULCINEE prediction capacity, in particular for neutronic kinetic aspects. The SPARTE tool includes surrogate models based on TRIPOLI4 calculations and experimental analysis. Several surrogate models were developed through the URANIE uncertainty platform (Gaudier, 2010) for ^{3}He depressurization, ^{3}He reactivity function of its density, including the "TOP effect", Doppler coefficient variation, neutron generation time, axial profile of neutron flux determination and rod drop reactivity insertion. Thus, for example, an artificial neural network surrogate model for the inserted reactivity was established from 750 TRIPOLI4 simulations taking as inputs: the control rods height, the ^{3}He density and the fuel temperature. More details on these surrogate models could be found in Clamens et al. (2018) and Clamens et al. (2019). These latter improvements allowed to better predict CABRI transients but its fault lies in the calculation of the injected reactivity which is uncoupled to the core calculation.

CATHARE (Code for Analysis of THermalhydraulics during an Accident of Reactor and safety Evaluation) is a two-phase thermal-hydraulic simulation tool in development since 1979 in France. The software is currently in its second major revision (CATHARE2) and is used, in particular, in pressurized water reactor safety analyses. The CATHARE2 tool has a modular structure capable of operating in 0D, 1D or 3D. It is able to model any type of reactor with several types of system loop. The software is based on a thermal-hydraulic two-phase model with six equations (conservation of mass, energy and momentum for each phase). This tool involves also a point-kinetic neutronic model and a thermomechanical model for the solid deformations computation. The

successive versions of the code were verified and validated in a two-step process: validation in separate-effect experiments followed by validation of the overall behaviour of the tool in integral experiments. Given its capabilities and its validation domain, this calculation tool has become in France the main thermal-hydraulic code for safety demonstration, and is widely used by the CEA, IRSN, EDF, Framatome etc.

2.3. CABRI RIA transient physics and analysis

2.3.1. Transient physics

Regarding the RI accidental sequences, external reactivity insertion induces strong temperature rises in the fuel pellets leading to very large radial thermal gradients and mechanical loads on the fuel and cladding which lead to structures expansion, fuel/clad gap evolution and pellet-clad interaction. The thermomechanical phenomena induce significant mechanical strain in the fuel pin and its cladding; involving changes in the pellet/clad heat transfers. More precisely, the heat transfers resulting from the nuclear power increase lead to clad and water temperatures rises. Consequently, reactivity feedbacks (Doppler effect, moderating effect, structures deformation) are efficient enough to lower the global reactivity and decrease the power, insuring the core integrity. Another multiphysic effect, called "TOP effect", can occur and acts in opposition of these feedbacks, being responsible of an increase of the power. In details, this effect is due to the (n;p) reactions in the transient rods of the type:

$$^{3}\mathrm{He} + \mathrm{n} \rightarrow \mathrm{p} + {}^{3}\mathrm{H} \quad (1)$$

The products of this reaction release their energy by collisions inside the rods, making the temperature and the pressure of the gas increase. Then, the ^{3}He density decreases locally, leading to a decrease of the absorption macroscopic cross section. This phenomenon makes the neutron flux and then the core power increase.

Looking at the key phenomena occurring during RI transients and presented on the phenomenological events tree in Fig. 2, one can note that these transients embrace thermal-hydraulics, thermomechanics and neutronics coupling.

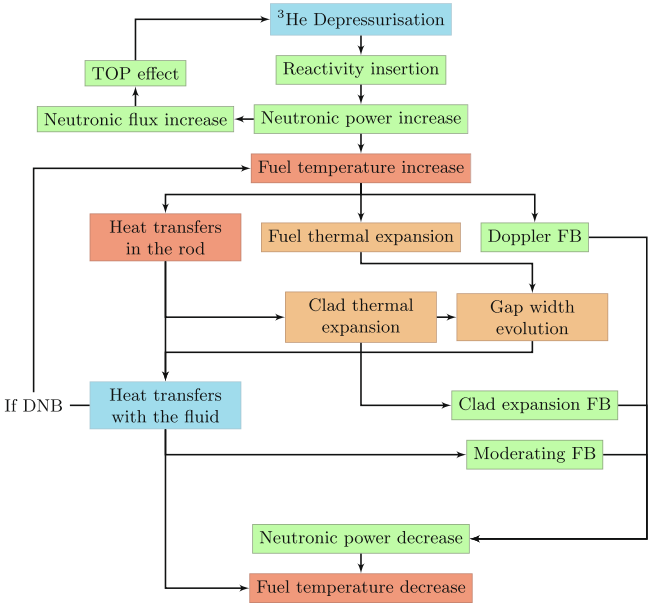

Fig. 2. phenomenological events tree of a RI transient in CABRI reactor neutronics in green, solid thermics in red, thermomechanics in orange and thermal-hydraulics in blue. FB: Feedback, DNB: Departure from Nucleate Boiling. (For interpretation of the references to color in this figure legend, the reader is referred to the web version of this article.)

2.3.2. QPIRT of CABRI transients

Based on this phenomenological events tree, the main physical phenomena have been identified. Following the PIRT methodology (Wilson and Boyack, 1998), the level of importance (High, Medium and Low) of each highlighted phenomenon in the final CABRI transient has been evaluated depending on the FWHM and the energy released inside the fuel; both variables featuring CABRI transients (cf. Table 1). The associated level of knowledge of each phenomenon and the level of uncertainty of its modelling have also been assessed in this table. This PIRT highlights phenomena deserving the greatest effort to improve its knowledge and modelling. These phenomena, which present a high importance, a low level of knowledge associated with a quite high uncertainty level on their models, are the Helium depressurization, the TOP effect and the heat transfers in the gap and to the fluid.

The "Quantified" step of this PIRT has consisted in temporally classifying the apparition of these phenomena during the transient and estimating the order of magnitude of the released energy required to observe a given phenomenon. The aim of this step, for validation purpose, is to separate physical phenomena whose orders of magnitude on the main transient parameters and times of occurrence are quite different. Analytical criteria have been defined for the energy deposit inside the core and its FWHM to distinguish CABRI transients and classify them in relation with the phenomenon to be validated. The characterisation of these separated effects leads to the classification of the CABRI experiment according to a two dimensional grid: in energy and in time (Labit et al., 2019).

By evaluating the characteristic time of radial conduction inside the pellet, the gap (filled with helium) and the clad and, finally, the characteristic time of convection into the flowing fluid, we obtain criteria on the FWHM of the power pulse that must be satisfied in order to expect these effects during the power pulse. They are listed in Table 2. When the power increases the fuel temperature rises, 150 ms after the clad starts heating and then, 120 ms later, the clad-to-coolant heat exchanges appear. The heat transfers in the coolant appear 120 ms after the clad heating, being 150 ms after the pellet heating. The neutronic phenomena can be considered as being instantaneous at the scale of the transient (being of the order of the neutron generation time, around 25 μs). These times have finally been reported in Table 1 to establish the occurrence time of each phenomenon from the beginning of the reactivity insertion, enabling to rank their apparition during the transient.

3. Validation methodology and available scientific calculation tools

3.1. Validation methodology

It can be derived from Table 2 that a pulse with a small FWHM can be used to validate the modeling of the Doppler effect. When this one is validated, a larger pulse can be considered in order to validate the thermal expansion effect etc. Second, orders of magnitude have been established considering the minimum energy at which each effect becomes significant for one transient power pulse. The chosen phenomena are the main feedbacks (Doppler effect and clad expansion effect) and the TOP effects for neutronics and the onset of nucleate boiling (ONB) in the coolant for thermal-hydraulics. Concerning feedback effects, the energy needed in order to obtain an averaged feedback reactivity greater than 10% of the maximum inserted reactivity is assessed. Concerning ONB, the criterion is obtained considering the energy required to bring the clad temperature to the fluid saturation temperature. For that, we assumed that the clad could be considered as thermally thin by calculating its Biot number: $B_i = e_c\ h_{conv}/\lambda_c \ll 1$. During fast transient power excursions, the ONB is quite delayed in comparison with slow transients. The wall temperature should reach the saturation temperature plus 40 °C (cf. Su et al., 2016b).

Concerning TOP effect, the energy needed in order to obtain a decrease of the ^{3}He density inside the rods leading to an increase of 10 %

Table 1
PIRT of CABRI RIA transients for short and long pulses (FB = feedback and Instant = Instantaneous).

	Importance according to energy deposit E						
Physical phenomenon	Low E	Medium E	High E	Very high E	Occurrence time	Level of knowledge	Level of uncertainty
Helium depressurization	H	H	H	H	Initiator	M	H
Reactivity insertion	H	H	H	H	Instant	H	L
TOP effect	L	L	H	H	Instant	L	M
Doppler FB	M	H	H	H	Instant	M	M
Clad expansion FB	L	Short : L	Short : L	Short : L	30 ms	M	M
		Long : M	Long : M	Long : H			
Moderating effect FB	L	L	Short : L	Short : L	150 ms	M	M
			Long : M	Long : M			
Solid heat conduction	M	M	H	H	30 ms (clad), 5 s (pellet)	H	L
Heat transfers in the gap	L	M	H	H	10 μs	M	H
Heat transfers to fluid	L	Short : L	H	H	150 ms	M	H
		Long : M					
Material deformations	L	L	H	H	30 ms (clad)	M	M

Table 2
Time criteria.

Effect	Time criterion
Fuel heating up Doppler effect	Instantaneous
Clad heating up and dilatation Clad expansion feedback	FWHM$\geq\tau_c$, $\tau_c = 30$ ms
Fluid heating up and eventually boiling Moderating effect feedback	FWHM$\geq\tau_c+\tau_{conv}$, $\tau_{conv} = 120$ ms

Table 3
Energy criteria.

Effect	Power criterion
Doppler feedback	$E \geq \rho_p c_{p_p}\left(\left(0.1\frac{\rho_{ext}}{A_{dop}}+\sqrt{T_0}\right)^2 - T_0\right)N_t\ h\ \pi r_p^2$
Clad expansion feedback	$E \geq \frac{1}{2\beta_c A}\ln\frac{c^2-(c^2-\pi r_{c_0}^2)\exp(-0.1\cdot\rho_{ext}/K)}{\pi r_{c_0}^2}\text{FWHM}$ $K = \frac{A_{mod}}{\beta_l}$ $A = \frac{\tau_c}{\rho_c c_{p_c}}\frac{2r_p\sqrt{\alpha_p\tau_c}-\alpha_p\tau_c}{N_t\ h\ \pi r_p^2}\frac{1}{r_{cext}^2-r_{cint}^2}$, $\alpha_p = \frac{\lambda_p}{\rho_p c_{p_p}}$
ONB in the coolant	$E \geqslant \rho_p c_{p_p}\left(T_{ONB}+\frac{h_{conv}}{h_{gap}}(T_{ONB}-T_\infty)\right)N_t\ h\ \pi r_p^2$ $T_{ONB} = T_{sat} + 40°\text{C}$ (cf. Su et al., 2016b) $T_\infty = 20°\text{C}$
TOP effect	$E \geqslant 10\%\frac{T_{He}(t_{pulse})}{B}$ $B = \frac{4}{15}\frac{\Phi_0}{P_{n_0}}\frac{N_A}{R}\sigma_{TOP}e_{TOP}$

of the external reactivity has been determined.

These criteria are presented in Table 3 as a function of parameters of interest of CABRI transients: energy deposit E, Full Width at Half Maximum (FWHM) and characteristic time of the effect (Labit et al., 2019). Henceforth, it is possible to discriminate transients in order to "filter" phenomena by choosing a transient with an energy deposit satisfying the previous criteria and a FWHM large enough to produce the effect wanted during the pulse.

These criteria allowed to build a validation map usefull to select transients for validation purpose. Existing CABRI transients of the commission tests (Lecerf et al., 2017) with their energy deposit, maximal external reactivity and FWHM (color of the point) are presented in Fig. 3. In the same figure, previously established criteria are drawn: Doppler criterion, clad thermal expansion criterion for a FWHM that is consistent with the characteristic time of the phenomenon (cf. Table 2), ONB criterion and TOP effect criterion.

From Fig. 3, we can deduce that almost every CABRI transients imply an important Doppler effect. Indeed, most available tests are situated above the curve representing Doppler criterion.

Concerning clad expansion feedback, available tests in which this effect can be noticeable during the pulse (effects near the criterion curve) have got a very little FWHM (around 10 ms). However, we have estimated (cf. Table 2) that the minimum FWMH in order to observe this effect during the pulse is 30 ms. From that, it can be deduced that the separated validation of these neutronic effects will be difficult if we only use the value of maximal power of the pulse as the main neutronic interest parameter. Dedicated CABRI transients should be performed with FWHM larger than 30 ms, or with a very late CSR (Control and Safety Rods) drop into the core in order to validate this feedback effect with the neutronic power after the pulse. The CSR drop should occur between 30 ms and 150 ms after the beginning of the pulse in order to avoid moderating effect (cf. Table 2).

The TOP effect criterion helps to identify transients that are likely to give a significant TOP effect. This criterion is quite consistent with the experimental observations, even if it under-estimates the energy deposit (experimentally around 100 MJ). This is due to the choice made for the establishment of the criterion, which considers the transient rods as a closed system during the time laps of the TOP effect. This can be valid if the characteristic time of the TOP effect (taken equal to the FWHM) is much lower than the depressurization duration. That way, the energy needed in order to generate a significant density variation in a closed system is necessarily lower than in an open system.

The last criterion seems to induce that the nucleate boiling will be difficult to see during CABRI transients, given that the energy deposit into the core is not high enough. As a consequence, every CABRI transient can be useful in order to validate single-phase transient heat transfer modeling. Nevertheless, we have demonstrated in Labit et al. (2020) that the impact of the choice of a heat exchange correlation on the temperatures is too weak to be validated against average measurement like the core outlet temperature.

This validation map then makes possible to identify physical models that could be validated against the power evolution and to select associated transients. The validation methodology that is developed is progressive and sequential:

- The reactivity insertion, without TOP effect, can be validated with transients R1, R2 and R3 (whose main parameters are given in

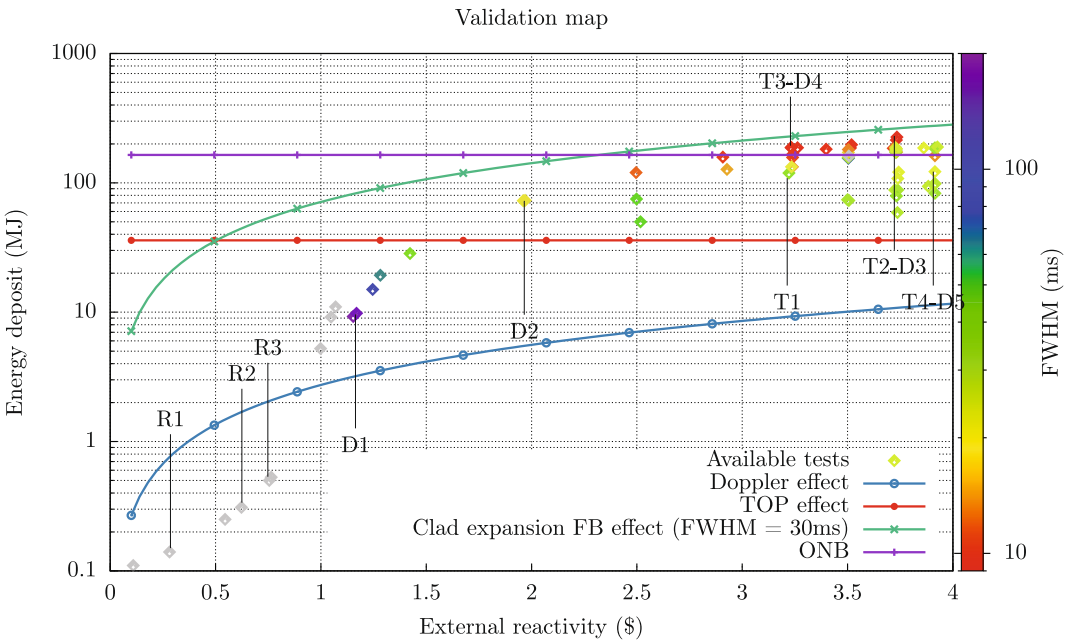

Fig. 3. CABRI commission tests and associated criteria enabling experimental validation of multiphysic modeling of RI transients (gray: undefined FWHM).

Table 4) and presented in Fig. 3 by comparison to the experimental neutronic power evolution. These transients will not induce feedback effects on the energy deposit. On a neutronic point on view, the reactivity insertion is the only effect that drives the power evolution in these transients. However, as the correct simulation of the reactivity insertion, and thus of the ^{3}He depressurization, is essential for the simulation of the transient in CABRI, the ^{3}He depressurization will be validated for each transient on another available data, which is the ^{3}He pressure evolution. Moreover, the ^{3}He reactivity model has been validated during steady-state experiments in the CABRI core for reactivities up to 4 $ (Clamens, October 2018). So once the kinetics of the insertion is validated in this step (that does not depend on the initial pressure), the validation of the reactivity insertion will be guaranteed for the whole range of CABRI experiments.

- The Doppler effect modeling will be validated on other CABRI transients (D1, D2, T2-D3, T3-D4 and T4-D5 – see Table 4) by comparison to the experimental neutronic power evolution. Indeed, looking at Fig. 3, it appears that Doppler effect could only be validated separately on CABRI tests presenting an energy deposit lower than 35 MJ (to remain below the TOP effect criterion). However, the Doppler model should be validated with several tests presenting a wide range of energy deposits to cover the CABRI physical domain. This neutronic effect is non-linear with the Doppler feedback coefficient and highly dependent on fuel temperature. Thus, it has been chosen to couple its validation with the TOP effect which mainly influences helium density (and not only the core power). Then, as the relation between the helium density and the reactivity has already been validated in the previous step with “R” transients without TOP effect, the TOP effect can be separately validated on the ^{3}He pressure evolution. This TOP effect induces, at the power peak, an additional ^{3}He pressure increase, which is compared between simulation and experiment for validation assessment. The TOP effect being validated, the validation of the Doppler effect modeling for energy deposit higher than 50 MJ could be pursued by comparing the simulations of neutronic power evolution with the experiments.
- In this manner, the TOP effect modeling will be validated with quite the same transients T1, T2-D3, T3-D4 and T4-D5 (see Table 4). This effect is thus validated independently of the Doppler effect, by comparison to the ^{3}He pressure measurement. These selected transients allow to validate both Doppler effect and TOP effect modelings. It is worth mentioning that ^{3}He flow is potentially sonic around the valves and largely compressible inside the transient rods. As its density varies much, temperature measurements should be performed in transient rods circuit in order to complete the validation of this ^{3}He flow behavior.

The main characteristics of the selected transients are summarized in Table 4. The validation is mainly based on the comparison of the simulations results with the measured evolution of the ^{3}He pressure and of the core power. The challenging goal of this sequential validation methodology is to validate, as much as possible, each effect separately. As the experimental uncertainties are sufficiently low (1 % for the ^{3}He pressure and 3 % for the neutronic power (Clamens et al., 2018), they do not jeopardize this validation methodology.

The level of knowledge of these major phenomena, leading to their proper modeling in various simulation tools, is also provided in Table 1 as well as the associated lacks. CATHARE2 being able to model all these phenomena, it has been chosen for the modeling.

3.2. An overview of the CATHARE2 code

CATHARE2 is a general simulation tool with validated models enabling the coupled simulation of phenomena of major importance for the CABRI transients (thermics, neutronics, single phase and two-phase flow thermal-hydraulics and thermomechanics). Nevertheless, the validation domain of CATHARE2 is rather different from the use domain associated to the CABRI transients. Some model improvements and additions of models are thus required based on the current CATHARE2 capability (Geffraye et al., 2011) for the simulation of the CABRI transients:

- neutronics taking into account 3D effects and improved feedback effects;
- the thermal-hydraulic wall to fluid heat transfers in very fast transient conditions and associated flow configurations;
- the thermomechanic effect of the pellet-clad gap evolution and its conductance;
- the ^{3}He depressurization through the modeling of the whole transient rods circuit and its regulating valves with sonic flows occurrence;

Table 4
Selected transients with main characteristics and effects modeling validation.

Transient	E (MJ)	FWHM (ms)	P_{He} (bar)	Type	h_{valve} (mm)	Validation
R1	0.14	Undefined	0.25	SD1	28.88	Depressurization (with ^{3}He pressure) and reactivity insertion (with power)
R2	0.31	Undefined	0.58	SD1	28.88	Depressurization (with ^{3}He pressure) and reactivity insertion (with power)
R3	0.53	Undefined	0.73	SD1	28.88	Depressurization (with ^{3}He pressure) and reactivity insertion (with power)
D1	9.26	165.8	1.20	SD1	28.88	Depressurization (with ^{3}He pressure) and Doppler effect (with power)
D2	72.8	18.0	2.60	SD1	28.88	Depressurization (with ^{3}He pressure) and Doppler effect (with power)
T1	119.0	33.5	7.00	SD2	3.81	TOP effect (with ^{3}He pressure)
T2-D3	226.0	9.1	11.50	SD1	14.16	TOP effect (with ^{3}He pressure) and Doppler effect (with power)
T3-D4	187.0	9.5	7.00	SD1	28.88	TOP effect (with ^{3}He pressure) and Doppler effect (with power)
T4-D5	122.0	20.0	14.50	SD2	5.33	TOP effect (with ^{3}He pressure) and Doppler effect (with power)

- the coupling between the core and the transient rods circuit: evolution of the external reactivity insertion with the multiphysic TOP effect.

These model improvements are given in Section 4. This gives rise to a new CATHARE2 version named CATHARE2 PALANTIR with new functions specific to RIA and CABRI reactor phenomena.

4. Multiphysic modeling of CABRI transients

The modeling of CABRI transients with the dedicated version PALANTIR of CATHARE2 has been developed to better manage and reproduce coupled multiphysic phenomena in CABRI reactor. It involves a coupling between the core circuit, which includes the nuclear core, and the transient rods circuit, whose depressurization leads to the reactivity insertion into the core. The main improvements of CATHARE2 in order to simulate the main physical phenomena, highlighted by the previous QPIRT (Section 2.3.2), are described in that section. They consist in neutronic (via neutronic feedbacks estimation), thermal-hydraulic and thermal-mechanic model improvements inside the core in the reactor circuit, and the modelling of the depressurization and ionisation of ^{3}He in the transient rods circuit.

The choice made in the representation of the core is a multi-1D modeling composed of 11 assemblies, with one hydraulic derivation per assembly (cf. Fig. 4 for the CABRI core schematizing and Fig. 5 for the CATHARE2 corresponding nodalization of the reactor circuit). As CABRI core being 2-planes symmetric, only a quarter of the core has been modeled. Thus the whole system gathering this multiphysic coupling is modeled in CATHARE2 PALANTIR: primary cooling system, CABRI pool and ^{3}He transient circuit, whose CATHARE2 nodalization is displayed in Fig. 6; the nodalization of the transient rods and the fuel rods of the core being identical and coupled. The bypass is modeled by contrast with the hodoscope channel and the reflector, whose neutronic influence is taken into account through radial and axial power profiles explained in the next section. Both Figs. 6 and 5 are of course not to scale in order to see every element.

The modeling improvements of the different physical domains for the reactor circuit focusing mainly on the core are described in Section 4.1 before presenting the modeling of the ^{3}He transient circuit (Section 4.2) and finally their coupling (Section 4.3).

4.1. CABRI core and reactor circuit

4.1.1. Neutronics

The evolution of power in the core in CATHARE2 is given by a point-kinetics method (Lamarsh, 1966), with 8 delayed neutrons precursor groups. The representation of the core in 11 assemblies allows taking into account specificity of each fuel assembly: radial and axial power profiles, radial and axial profiles of feedback effects and the number of fuel rods. Indeed the neutronic power distribution in not flat as it is illustrated in Fig. 4 (Labit et al., 2019). Even if this method does not allow to simulate radial and axial profiles or neutron spectrum evolutions during the transient, all major feedback effects are computed in a 3D way with a differential method. This consists in a preliminary improvement of the neutronic method. Nevertheless, work is underway to evaluate the results discrepancy with a new kinetic neutronic method in TRIPOLI (Faucher et al., 2018). Depending on that, a 3D coupling between CATHARE2 PALANTIR and TRIPOLI might be envisaged. But currently, the improved kinetics method will be considered to obtain global results on CABRI.

Feedback effects taken into account are Doppler effect ρ_{dop}, feedback linked to the moderator ρ_{mod} (thermal expansion and vapour generation), and expansion of the clad ρ_{dil} that reduces the moderator ratio. The Monte-Carlo code TRIPOLI4 (Brun et al., 2011) with the JEFF3.1.1 nuclear data library (Santamarina et al., 2009) is also considered to provide radial and axial power profiles to this CATHARE2 modeling for each initial state. An example of axial profile and radial power distribution is presented in Fig. 4.

Given that the kinetics of these transients is very fast, the computation of reactivity should manage feedback coefficients variations. That way, differential methods are chosen rather than integral methods. It consists in calculating the contribution of every feedback effects between $t-\dot{t}$ and t before being integrated between 0 and t. This is explained in Eq. (6).

$$\rho_{fb} = \int_0^t \delta\rho_{fb} = \int_0^t \mathrm{A}_{fb}(t')\frac{\mathrm{d}\chi(t')}{\mathrm{d}t'}\mathrm{d}t' \tag{2}$$

Where χ is the scalar function governing the insertion of anti-reactivity ρ_{fb}, A_{fb} is the coefficient of feedback effect. This computation is made for each axial mesh of each fuel assembly. The equations below describe the way feedback effects are computed for the assembly i.

$$\delta\rho_{mod_i} = \frac{N(i)}{N_t}F_{xy_{mod}}(i)\sum_{i_z=1}^{N_z}F_{z_{mod}}(i)\frac{\mathrm{A}_{mod}}{\rho_l(t;i_z)\beta_l(t;i_z)}((1-\alpha(t;i_z))\mathrm{d}\rho_l(t;i_z) - \mathrm{d}\alpha(t;i_z)\rho_l(t;i_z)) \tag{3}$$

Eq. (7) models the moderator feedback reactivity, that can be simplified with $(1-\alpha)\mathrm{d}\rho_l - \mathrm{d}\alpha\rho_l = \mathrm{d}\rho_f$. This is true when vapour

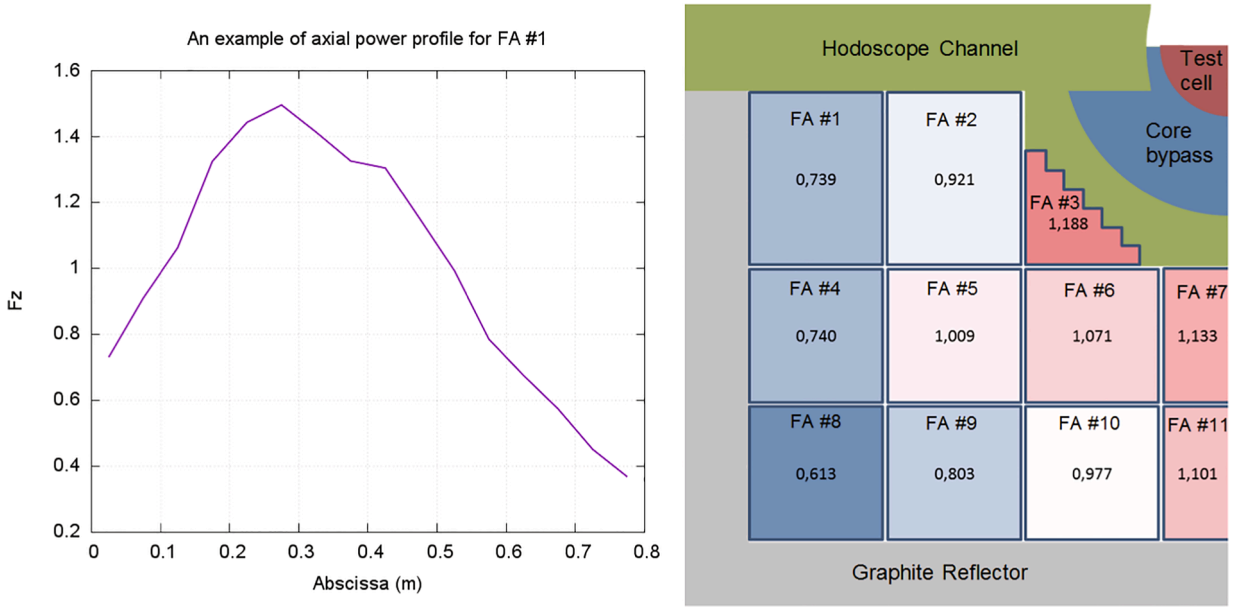

Fig. 4. left: an example of axial power profile F_z for assembly FA♯1 right: core modeling with average radial power coefficients $< F_{xy} >$.

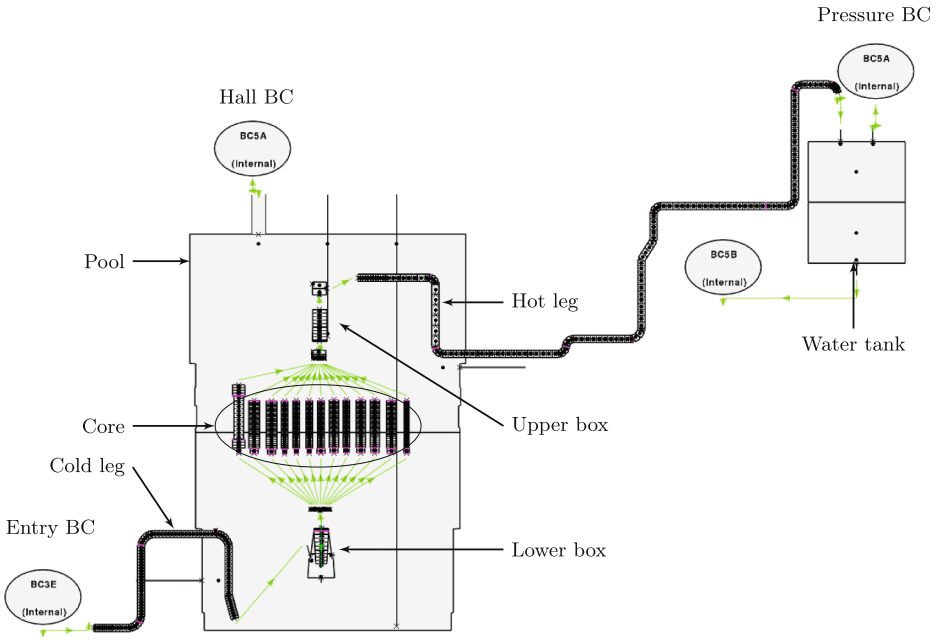

Fig. 5. CATHARE2 nodalization of the core circuit.

temperature is equal to saturation temperature and $\rho_v \ll \rho_l$. These hypotheses are valid until departure from nucleate boiling. Eq. (8) gives the model of differential anti-reactivity due to the expansion of the clad implemented in PALANTIR.

$$\delta\rho_{dil_i} = \frac{N(i)}{N_t} F_{xy_{dil}}(i) \sum_{i_z=1}^{N_z} F_{z_{dil}}(i) \frac{\mathrm{A}_{mod}}{\beta_l(t;i_z)} \frac{2\pi r_{c_{ext}}(t;i_z)\mathrm{d}r_{c_{ext}}(t;i_z)}{c^2 - \pi r_{c_{ext}}^2(t;i_z)} \tag{4}$$

where $r_{c_{ext}}$ is the external radius of the rod, N_z is the total number of axial meshes in the fuel rod.

In the case of the Doppler effect, contributions of each radial mesh of each axial mesh in the pellet are weighted, summed and integrated over the whole core.

$$\delta\rho_{dop_i} = \frac{N(i)}{N_t} F_{xy_{dop}}(i) \sum_{i_z=1}^{N_z} F_{z_{dop}}(i) \sum_{i_r=1}^{N_r} \mathrm{A}_{dop} \left(\sqrt{T(t;i_z;i_r)} - \sqrt{T(t-\mathrm{d}t;i_z;i_r)} \right) \frac{V_m(t;i_z;i_r)}{V_i} \tag{5}$$

where N_r is the total number of radial meshes in the fuel rod, V_m and V_i are respectively the volume of the mesh and the total volume of the fuel assembly. In Eq. 9, A_{dop} depends on the fuel temperature T, the ^{3}He density and the position of the control rods. A surrogate model takes this variation into account during the computation (Clamens et al., 2018). $F_{xy_{dop}}$ and $F_{z_{dop}}$ are respectively radial and axial Doppler profiles. By using the perturbation theory (Lamarsh, 1966), it has been analytically demonstrated that these coefficients could be approximated by radial

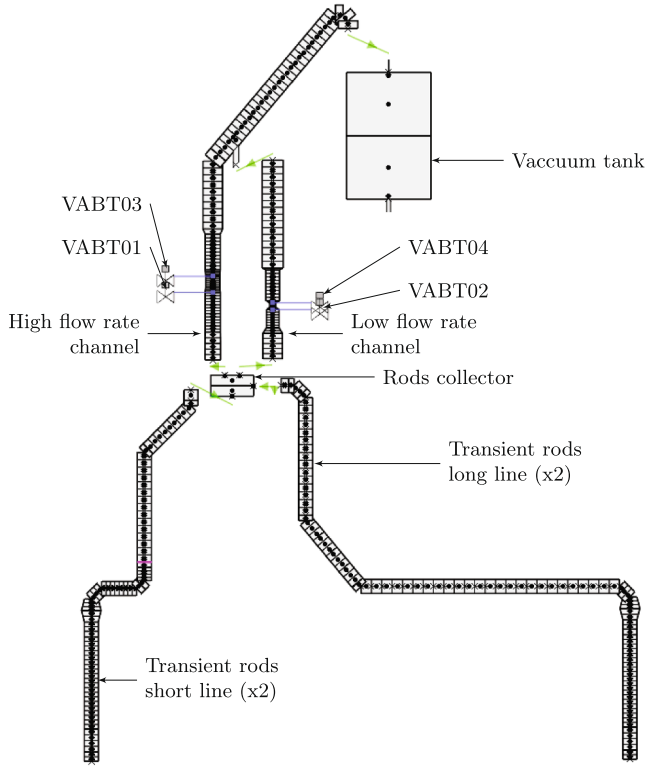

Fig. 6. CATHARE2 nodalization of the transient circuit.

and axial power profiles: $F_{xy_{dop}} \propto F_{xy}^2$ and $F_{z_{dop}} \propto F_z^2$. Rigorously, other feedback effects are also weighted by specific radial and axial profiles, as it is done for Doppler effect. Nevertheless, their relations have not been analytically established yet and a weighting in $F_{xy_{fb}} \propto F_{xy}^2$ and $F_{z_{fb}} \propto F_z^2$ is considered.

In addition to that, external reactivity ρ_{ext} is determined by computing ^{3}He rods depressurization in the transient rods circuit (described in Section 4.2). The control rods reactivity evolution during the scram is also modeled in PALANTIR and contributes to ρ_{ext}.

4.1.2. Thermal-hydraulics

The geometry of the lower and upper parts of the fuel assemblies and thus the rod bundles heating perimeters vary among the various assemblies of the CABRI core. These features, in addition with different axial and radial power profiles, lead to different axial pressure losses and ratios of assembly power over its flow rate. The Reynolds number *Re* and so the Nusselt number *Nu*, governing the heat exchange coefficient correlations, depend on the assembly. Firstly, the thermal-hydraulics modeling of the CABRI core has consisted in calculating singular pressure loss coefficients in the lower and upper parts of each assembly (Idel'Cik, 1960).

The choice of modeling CABRI core with one 1D-hydraulic derivation per assembly prevents the computation of 3D flows. An estimation of possible 3D flows has been made, studying the effects which should induce radial heat, mass and momentum transfers between assemblies (Labit et al., 2019). These effects could be due to:

- large radial temperature differences between assemblies inducing heat exchanges in a pure heat conduction way in the fluid. Estimation studies have concluded that this effect would be smaller than the one caused by the viscous diffusion;
- radial differences of velocity between assemblies causing momentum exchanges due to viscosity. This effect has also been estimated to be negligible in an extreme case presenting a velocity ratio of 5 between assemblies;
- radial differences of pressure, density or velocity between assemblies, creating radial mass and energy exchanges in the core, known as "crossflows".

The analytical calculation of orders of magnitude of the first two effects revealed that these phenomena are very negligible even in RI transients, having respectively no impact on the mean temperature and the mean velocity. However, the third effect is much more complex and the effect of huge radial differences of density is not necessarily negligible (Labit et al., 2019); the estimated radial velocity can reach $v_r \sim 0.7$ m/s when axial velocity is $v_z \approx 5$ m/s. These "crossflows" are thus estimated as 10 % of the mean axial flow rate. This point will be investigated in a near future to check if this last effect is sufficient to affect the results. Sensitivity studies would be carried out using the 3D thermal-hydraulic module of CATHARE2 for the simulation of the CABRI core.

Furthermore, an important point which is worth mentioning is that, in CATHARE2, the convective heat exchange coefficients are validated and qualified on quasi-steady experiments (Geffraye et al., 2011) only, as in most thermal-hydraulic tools. These transient convective heat exchange coefficients in single and two-phase flow regimes are not qualified, when characteristic time of the wall heat flux increase is around the millisecond. The kinetics of such a transient is so fast that the usually used steady-state models reach their validity limits and it has been noticed that transient heat exchange coefficients can be much larger in fast transients (Visentini et al., 2014). Single phase convective heat exchange coefficient correlation has been modified in CATHARE2 PALANTIR according to a recent work (Labit et al., 2020). The single phase pure convection is the overlap of two main mechanisms: the advection (wall axial supply in upstream cold water) and the turbulent mixing in the boundary layer. This latter phenomenon is due to vortexes in the boundary layers inducing radial mixing through the velocity boundary layer. In CABRI conditions, the turbulent mixing phenomenon is preponderant over the advection. To these mechanisms is added a pure conduction heat exchange mechanism through the thermal boundary layer. Convection and conduction overlap in order to give a conducto-convective heat transfer coefficient, improperly called "convection" coefficient only. Considering that the normalized heat transfer coefficient is conveniently correlated by the non-linear superposition method as in Su et al. (2016a, 2016b), we can obtain:

$$\overline{h} = \sqrt[n]{1 + \left(\frac{h_{cond}}{h_{st}}\right)^n} \tag{6}$$

where h_{cond} is the pure conduction heat transfer coefficient and h_{st} is the conducto-convective heat transfer coefficient in steady-state. $\overline{h}$ is the normalized heat transfer coefficient with:

$$\overline{h} = \frac{h_{tr}}{h_{st}} \tag{7}$$

where h_{tr} is the conducto-convective coefficient during fast transient excursions, that shall be determined. The coefficient in steady-state is derived from Sieder-Tate's correlation whereas h_{cond} is obtained by solving the transient conduction equation in the fluid, thanks to Laplace transform method (Labit et al., 2020), for an exponential heat flux proportional to $e^{t/\tau}$ where τ is the excursion period. This leads to:

$$h_{tr}(t,\tau) = \left(1 + \left(\frac{\lambda}{\sqrt{\alpha_l \tau}\,\mathrm{erf}\left(\sqrt{t/\tau}\right) h_{st}}\right)^n\right)^{1/n} h_{st} \tag{8}$$

According to Eq. (8), the transient conduction becomes preponderant for low power excursion periods whereas forced convection governs heat transfers at high periods (the heat flux excursion periods in CABRI

tests range between 10^{-3} s and 10^{-1} s). n has been taken equal to 2.4 ± 0.6 in Labit et al. (2020) based on experimental data (Su et al., 2016b).

Finally, the transient single phase coefficient given in Eq. (8) has been validated in Labit et al. (2020) with separate effect tests results from Su et al. (2016a, 2016b). It has been implemented in CATHARE2 PALANTIR with τ evaluated during the simulation for each axial mesh in each hydraulic derivation.

4.1.3. Thermal-mechanics

Thermal coefficients (conductivity, heat capacity, density) of the fuel structures, that are used, are determined with usual laws (Laurent and Vuillermoz, 1993). Additional measurements performed on a CABRI hot rod in CEA Cadarache nuclear center allowed to validate these laws for CABRI fuel and to determine the fuel porosity. Before the power excursion, the thermal-mechanic steady-state is calculated for each assembly.

The CATHARE thermal-mechanic module simulates different phenomena:

- cladding creep;
- thermal expansion of structures (pellet and clad);
- elastic strain of the clad due to the difference of pressure between coolant and pellet-clad gap.

From the evaluation of the orders of magnitude of these various terms, it has been demonstrated that the thermal expansion mechanism is the prominent effect and that the yield strength is not overtaken in core pins, even in CABRI RIA conditions. Using this module, the evolution of the pellet/clad gap closure in fuel rods is simulated. The heat exchange coefficient in this gap during the transient is the sum of a radiative and a conductive exchange. The conductive heat exchange coefficient for each axial mesh in each fuel assembly, is given by Eq. (9) as long as this gap is opened (*i.e.* larger than 1.5 μm), assuming low burn-up and thus pure helium gas:

$$h_{gap}(t) = \frac{\lambda_{He}(T_{He})}{e_{gap}(t) + \overline{l_c} + \overline{l_g}} \tag{9}$$

where $\overline{l_c}$ and $\overline{l_g}$ are extrapolation distances taking into account the fact that the mean free path of the gas particles can be lower than the gap thickness itself (Lassman and Hohlefeld, 1987). When the gap is closed, Eq. (9) is no more valid and is replaced by a model (Lassman and Hohlefeld, 1987), implemented in CATHARE2 PALANTIR, where the bulk heat transfer coefficient h_{gap} consists in the sum of a radiation component, a gap component dependent on gas and surface characteristics, and a contact term component dependent on the contact pressure. An analytical expression of the contact pressure between the pellet and the clad (Lamkin, 2017) has thus been also added in CATHARE2 PALANTIR in order to calculate at each time step the contact pressure for each axial mesh.

4.2. The ^{3}He transient rods circuit

The CABRI transient rods circuit, which is composed of four transients rods linked to a tank by two channels, has also been modelled with CATHARE2 PALANTIR. Outside thermal exchanges have been added and a specific fluid (^{3}He) has been created with its given purity (volumic amount of pure ^{3}He in the gas composition). A theoretical work has led to the modeling of the compressible flow of ^{3}He in the transient rods circuit during the depressurization and more precisely throughout the valves. The determination of the control valves features has been an important part of this work: the valve capacity (C_v) and the maximum admissible pressure drop ratio (x_T).

4.2.1. Valve capacity

Each valve has thus been characterized. The mass flowrate of gas crossing a valve is, according to Masoneilan standards (Masoneilan, 1998):

$$Q_m = kC_v Y(x)\sqrt{xP_0\rho_0} \tag{10}$$

P_0 and ρ_0 are pressure and density at upstream conditions. k is a conversion coefficient from imperial units to international system units. $Y(x)$ is a function taking into account the compressibility of the gas when the pressure drop is increasing and C_v is the capacity of the valve. x is the pressure drop ratio across the valve, equal to $\min(x_T; \Delta P/P_0)$. x_T is specific to the valve, standing for the pressure drop at which the flow becomes sonic. A correlation of the pressure loss coefficient across the valve is issued from Idel'Cik (1960). Then, the valve capacity and the pressure loss coefficient have been related this way:

$$C_v = Q_{U.S.gal/min}\sqrt{\frac{\rho_{^3\mathrm{He}}/\rho_{water}}{\Delta P_{psi}}} = \frac{1}{k}\sqrt{\frac{2}{\xi}}\frac{\pi}{4}D_0^2 \tag{11}$$

ξ depends on the opening of the valve and D_0 is the hydraulic diameter of the upstream pipe. If h is the position of the control valve stem, then:

$$\xi = 0.6 + 0.15\left(\frac{D_0}{h}\right)^2 \tag{12}$$

4.2.2. Maximum admissible pressure drop ratio

The x_T parameter is also dependent of the opening of the valve, which is characterized by the valve stem position (h_{valve}). It has been determined by comparing results of an analytical model (based on a Joule & Gay-Lussac expansion) to 16 discharge experiments on the transient rods circuit, for different apertures. These discharge experiments were performed in the framework of the commissioning of CABRI's valves of the transient circuit. They cover the various types of ^{3}He depressurization, realized on CABRI, with a large range of pressure (7–14.7 bar) and different valve openings (valve stem position from 2.6 to 28.88 mm).

In that purpose, a simplified situation, where two volumes are connected by a "ponctual" valve, has been considered. Initially, the pressure is fixed to test condition upstream of the valve and the void pressure (5 mbar) is fixed in the discharge tank. The discharge is adiabatic to be close to Joule & Gay-Lussac expansion situation, and the gas is assumed to be ideal. Final values of x_T, according to the stem valve position, have been determined for the two control valves (VABT03 and VABT04 see Fig. 6). These two laws of x_T have been then implemented in the PALANTIR model.

4.3. Reactor and transient rods circuits coupling

After the modeling of the whole transient rods circuit, this one has been coupled with the reactor circuit: heat exchanges between the primary cooling system and the transient rods circuit and gas ionization have been modeled. This last development made it possible to compute the external reactivity insertion during the transient and to take into account the so-called "TOP effect" (Clamens et al., 2018). This effect, due to helium ionization, making the temperature increase and the density decrease, impacts the global core neutronics: $^3\mathrm{He} + n \longrightarrow {}^3\mathrm{H} + p$. This reaction adds a volumic power inside the transient rods, that has been modeled this way (Labit et al., 2019):

$$p_v(x,y,z,t) = F_{xy}F_z\frac{\Phi_0}{P_{n_0}}P_n(t)\rho_{\mathrm{He}}(z,t)\frac{N_A}{M_{\mathrm{He}}}\sigma_{TOP}\ e_{TOP} \tag{13}$$

σ_{TOP} is the microscopic cross section of TOP reaction $^3\mathrm{He}(n;p)^3\mathrm{H}$ and e_{TOP} the energy released by such a reaction (Rondeaux, 2011).

The linear relation between neutron flux and power is consistent with point kinetics model. Φ_0 and P_{n_0} are respectively the neutron flux and the associated power at the criticality. $F_{xy}F_z\Phi_0/P_{n_0}$ is given by

TRIPOLI4 evaluations, F_{xy} and F_z being respectively radial and axial flux coefficient in the transient rods. Moreover, CATHARE2 PALANTIR computes the power evolution at each time step $P_n(t)$ and the helium density inside the rods $\rho_{He}(z,t)$.

Finally, the relation between the density of helium in the rods, calculated by CATHARE2 PALANTIR, and the external reactivity is given by a surrogate model, established with URANIE and TRIPOLI4 (Clamens et al., 2018.

5. Multiphysic validation results

To validate this multiphysic modeling in CATHARE2 PALANTIR of the CABRI reactor, Best-Estimate results of some selected transients (cf. Fig. 3 and Table 4) are compared to experimental results.

Every initial state has been computed with TRIPOLI4.9 to provide radial and axial power distributions to the CATHARE2 PALANTIR multiphysic modeling.

The models presented in this paper that will be validated are:

- the computation of the external reactivity thanks to the helium depressurization,
- the Doppler feedback modeling,
- the ^{3}He depressurization,
- the TOP effect.

5.1. Validation of the reactivity insertion modeling and kinetic parameters

Results are presented in Fig. 7. Each graph gathers the ^{3}He pressure and the neutronic power evolutions. Dash lines present the experimental results and plain ones the simulation results.

Red curves are related to the core fission power and green ones to the ^{3}He pressure. The orders of magnitude of the experimental uncertainties are 1% for the ^{3}He pressure and 3% for the neutronic power (Clamens et al., 2018). Error bars are small.

The results obtained with this modeling are satisfactory, in spite of the slight underestimating of the pulse height. This can be explained by the final ^{3}He pressure that is not well reproduced by the modeling, that is a consequence of the fact that CATHARE2 does not accept helium pressure under 17.5 mbar (contrary to the experiment where the void can be set under 5 mbar). In addition, those comparisons show that the calculated CSR scram is slightly faster than the experimental one.

The transients R1, R2 and R3 give a very good consistency with the experiment, and a neutronic power predicted at −5 % by the modeling. The helium depressurization and the reactivity insertion are validated with these Best-Estimate results.

5.2. Validation of the Doppler feedback effect modeling

Results of transients D1 and D2 are presented in Fig. 8. The results obtained for transients D1 and D2 are satisfactory. The simulated evolution of the Helium pressure and of the core power are in good agreement with the measured data. The total energy released is predicted at 10% for D1 and 7 % for D2. The FWHM and the instant of the peak power are well simulated. The maximum power is predicted at 5 % by the simulation for D1. Despite this overall fairly good consistency, the simulation of the transients D2 leads to 21% of difference on the maximal neutronic power. This difference could not be only attributed to the Doppler feedback effect modeling. Indeed, further sensitivity studies have highlighted that the initial value of the fuel/clad gap width, valve parameters or ^{3}He purity highly influence the power pulse. Taking into account the modelling uncertainties would lead to approximately 10% uncertainty on the deposited energy and the maximum power (Clamens, October 2018). At this step, it is still difficult to guaranty the validation by applying the validation methodology proposed in Section 3.1 based on Best-Estimate simulations. In the future, this methodology will be performed based on Best-Estimate Plus Uncertainty simulations taking into account the uncertainties linked to the different parameters

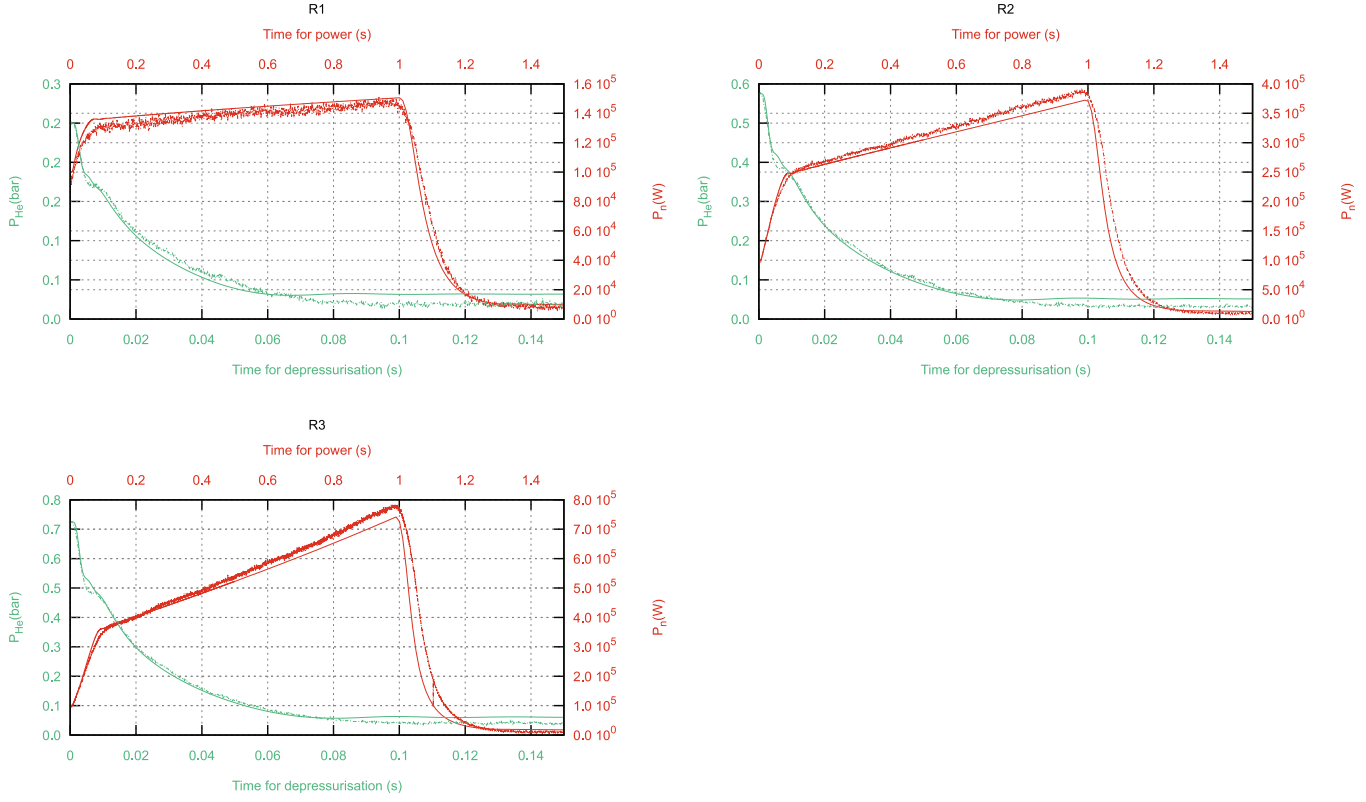

Fig. 7. Comparison of results for transients R1, R2 and R3.

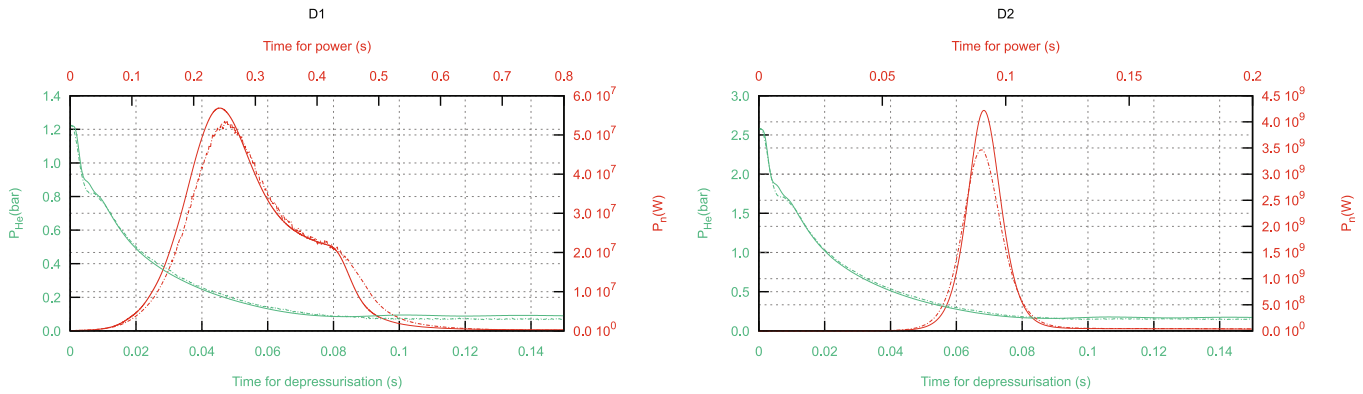

Fig. 8. Comparison of results for transients D1 and D2.

(such as this gap width, valve parameters, gas purity etc.), or linked to the models as well as the experimental uncertainties, similarly to what is done in Seiler-Marie et al. (2019).

Concerning the depressurization, the effect of the bad value of the initial pressure in the vacuum tank is no more significant given the initial high pressure difference between rods and tank.

5.3. *Validation of the TOP effect and the Doppler effect modeling for highly-energetic pulses*

Results devoted to this validation are presented in Fig. 9. Transient T1 leads to a non-negligible TOP effect during the computation of the pulse with CATHARE2 PALANTIR. But the TOP effect detected during the experiment is not as important as it is with the computation. This discrepancy leads to an important difference between the computed and experimental pulses. This lack allowed to identify that, even if the pressure evolution is correct, the temperature evolution in the helium rods is not. This is due to the fact that during SD2 (slower depressurization), the flow is laminar in the rods, because the flow rate in the valves is very low, in comparison with SD1 (faster depressurization). However, the correlations used in CATHARE2 PALANTIR for laminar gas flows are not accurate enough and adapted to this situation. This will be modified in a near future. In spite of this, results for other transients are very satisfactory, including SD2 (T4-D5) with large valve openings. The helium depressurization is quite well computed (by comparison of experimental and computed pressure "bumps" during the pulse). A slight delay of the pulse is observed during transient T4-D5. For the same reason as before, the helium density decrease dynamics is not well

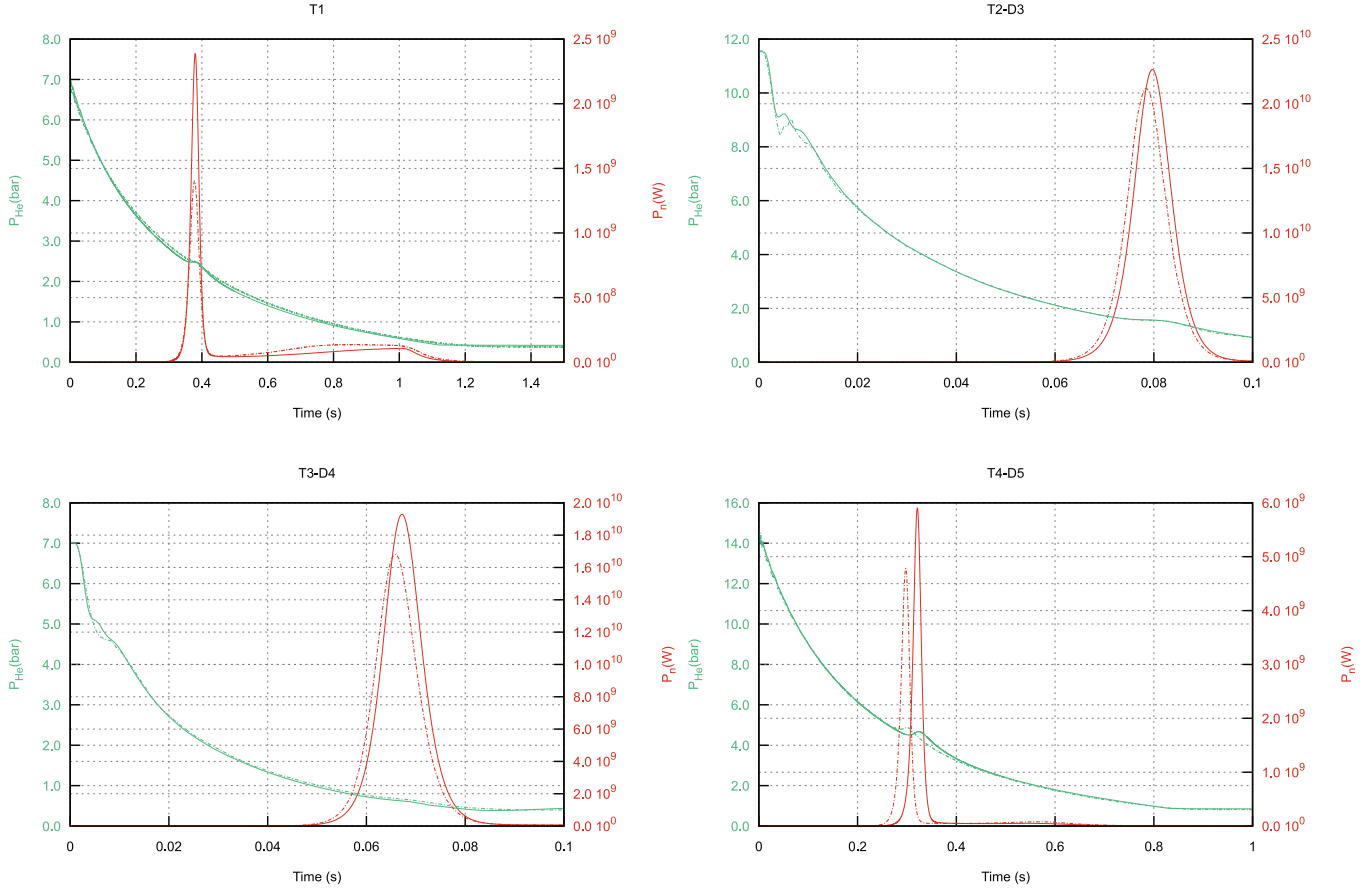

Fig. 9. Comparison of results for transients T1, T2-D3, T3-D4 and T3-D5.

computed for SD2.

For transients T2-D3, T3-D4 (where TOP effect is correctly computed), the maximal power is very well predicted by the modeling (+15% over the experimental power). We conclude that the Doppler effect feedback modeling that has been developed allows to compute a power pulse (when no more neutronic feedback effects are overlapping) at 15% close to the experimental data.

5.4. Discussion

The validation results are summarized in Table 5 showing the discrepancies between the calculations and the experiments; the calculated ratio is (computed-experiment)/experiment.

One can deduce that the depressurization is rather well computed by CATHARE2 PALANTIR, even if we notice important discrepancies for transients with low initial pressures, that are due to a numerical limitation of the initial pressure in the vacuum tank (17.5 mbar). Then, the reactivity insertion is validated on transients R1, R2 and R3 with the power, predicted at ±4%. The Doppler effect modeling accuracy is verified on power evolution, predicted at ±20% close to the experiment for transients D1, D2, T2-D3, T3-D4 and T4-D5. Transients T1, T2-D3, T3-D4 and T4-D5 present non-negligible TOP effects, well predicted for every transient except T1, where the "pressure bump" corresponding to the TOP effect during the pulse is too high. This is at the origin of a core power overestimation. Some investigations help us concluding that these bad results are due to a lack in the definition of the laminar Nusselt number in the rods. As a consequence, even if the TOP effect seems to be well modeled, for a low valve aperture the depressurization (and especially the density evolution) is not, *i.e.* for transients with compressible laminar flows in the transient rods.

Table 5
Computation – experiment discrepancies of interest parameters for selected transients.

Transient	Maximal power discrepancy	Released energy discrepancy	FWHM discrepancy	Helium pressure maximal discrepancy
R1	+3 %	+0.5 %	Undefined	+56 % (final pressure)
R2	−4 %	−6 %	Undefined	+50 % (final pressure)
R3	−3 %	−5 %	Undefined	+25 % (final pressure)
D1	+5 %	+10 %	−0.1 %	+20 % (final pressure)
D2	+21 %	+7 %	−10 %	+20 % (final pressure)
T1	+70 %	−7 %	−23 %	+6 %
T2-D3	+7 %	+2 %	−4 %	+6 %
T3-D4	+15 %	+21 %	−4 %	−8 %
T4-D5	+22 %	+15 %	−2 %	+6 %

6. Conclusion and prospects

This paper has presented an improved multiphysic modeling of the CABRI-RIA transient with the CATHARE2 tool, an experimental validation methodology of this tool and a preliminary practical application of this methodology.

The objectives were first to identify the main phenomena during a RIA with a QPIRT and then to suggest a way to model them with a calculation tool. This tool, CATHARE2 PALANTIR, is a specific version of CATHARE2 that has been developed in order to model the reactivity insertions in nuclear reactors on a multiphysic way. It is able to take into account thermal-hydraulic, neutronic, thermal-mechanic effects and the coupling of these domains. Hence, a validation methodology was build in order to validate the physical models added into this tool. The capabilities of this tool have been tested over the CABRI experiments, highlighting a very good consistency of the results. This sequential and progressive validation methodology would be soon extended to Best-Estimate Plus Uncertainty simulations; taking into account the input parameters and models uncertainties.

In spite of these promising results obtained with Best-Estimate simulations, some lacks have been identified during the application of the validation methodology and are now under development in PALANTIR:

- the wall to fluid heat transfers in the helium rods are insufficiently defined for laminar flow in the rods, i.e. for low valve openings in SD2;
- the vacuum initial pressure is too high and leads to important discrepancies on the final pressure for low initial helium pressures;
- the model uncertainties impact will be studied in a near future via uncertainties propagation with URANIE (Gaudier, 2010) and confronted to the experimental measurements and their associated uncertainties. In the future, this methodology would be applied based on Best-Estimate Plus Uncertainty simulations which would also take into account the uncertainty linked to some experimental and model parameters.

In absolute terms, additional measurements would be needed in the CABRI reactor in order to validate other phenomena modelling:

- helium temperature in the transient rods for a complete validation of the depressurization;
- clad temperature measurements in the core for a more accurate validation of the transient heat exchange modeling.

In that purpose, additional experiments should be performed too. Very large pulses or pulses with a late control rods drop into the core, with an energy deposit high enough to satisfy clad expansion criterion, are necessary to validate the clad expansion and the moderator feedbacks modelings.

The Best-Estimate modeling might also be improved in order to take into account for instances cross-flows in the core with a 3D thermal-hydraulics modeling, spectrum and power shape evolution with a 3D kinetics method. The outcome of such improved multiphysic models might be benefit to the industry and the regulatory bodies as well as to improve the design/operating conditions of nuclear reactors. This work will contribute to new advancing in the multiphysic simulations of fast transients caused by reactivity insertion.

CRediT authorship contribution statement

J.-M. Labit: Writing - original draft, Writing - review & editing, Methodology, Formal analysis. **N. Marie:** Writing - original draft, Writing - review & editing, Methodology, Supervision, Formal analysis. **O. Clamens:** Writing - review & editing, Methodology, Supervision. **E. Merle:** Writing - review & editing, Data curation.

Declaration of Competing Interest

The authors declare that they have no known competing financial interests or personal relationships that could have appeared to influence the work reported in this paper.

Acknowledgements

The authors would like to thank the IRSN, EDF and Framatome contributing to the study financing.

References

Brun, E., Dumonteil, E., Hugot, F.-X., Huot, N., Jouanne, C., Lee, Y.-K., Malvagi, F., Mazzolo, A., Petit, O., Trama, J.-C., et al., 2011. Overview of TRIPOLI-4 version 7, Continuous-energy Monte Carlo Transport Code. In Proceedings of ICAPP 2011.

Clamens, O., Blaise, P., Hudelot, J.-P., Lecerf, J., Duc, B., Pantera, L., Biard, B., 2018. Coupled experimental and computational approach for CABRI power transient analysis. IEEE Transactions on Nuclear Science 65 (9).

Clamens, O., Lecerf, J., Hudelot, J.-P., Duc, B., Blaise, P., Biard, B., 2018. Modeling of the ^{3}He density evolution inside the CABRI transient rods during power transients. IEEE Transactions on Nuclear Science 65 (9), 2510–2517.

Clamens, Olivier, Hudelot, Jean-Pascal, Blaise, Patrick, 2019. Analysis of the doppler feedback reactivity in LWR power transients - application to the CABRI reactor. In: Proc. Int. Conf. ICCAP2019, JuanlesPins, France.

Clamens, O., 2018. Analyse et propagation des incertitudes associées à la dépressurisation de l'Hélium 3 sur les transitoires de puissance du réacteur CABRI. PhD. Thesis report, October 2018.

D'Auria, F., Salah, A.-B., Giorgio, G., et al., 2004. Neutronics/thermal-hydraulics Coupling in LWR Technology, Vol. 1 CRISSUE-S. OECD/NEA ISBN 92-64-02083-1, Paris.

Faucher, M., Mancusi, D., Zoia, A., 2018. New kinetic simulation capabilities for tripoli-4: Methods and applications. Annals of Nuclear Energy 120, 74–88.

Gaudier, F., 2010. URANIE: The CEA/DEN uncertainty and sensitivity platform. Procedia - Social and Behavioral Sciences 2 (6), 7660–7661.

Geffraye, G., Antoni, O., Farvacque, M., Kadri, D., Lavialle, G., Rameau, B., Ruby, A., 2011. CATHARE 2 V2.5_2: A single version for various applications. Nuclear Engineering and Design 241 (11), 4456–4463.

Hudelot, J.-P., Fontanay, E., Molin, C., Moreau, A., Pantera, L., Lecerf, J., Garnier, Y., Duc, B., 2016. CABRI facility: upgrade, refurbishment, recommissioning and experimental capacities. In: Proc. Int. Conf. PHYSOR2016, Sun Valley, USA.

Idel'Cik, I.E., 1960. Spravotchnik po guidravlitcheskim soprotivleniam. Gosenergoizdat Moscow, USSR.

Jeury, F., Pantera, L., Garnier, Y., 2013. CABRI Experimental Reactor: Experimental Reassessment of CABRI Core Power and Measurement Uncertainties. Proc. Technology Mtg. IGORR 2013, 13–18.

Labit, J.-M., Marie, N., Hudelot, J.-P., Merle, E., 2019. An advanced experimental validation methodology of multiphysics calculation tools on CABRI transients. In: Proceedings of M&C 2019, volume 1, pages 2684–2695, Portland, Oregon, August 2019.

Labit, J.-M., Marie, N., Merle, E., Clamens, O., 2020. Transient heat exchanges under fast reactivity insertion accident. Nuclear Engineering and Design.

Lamarsh, John R., 1966. Introduction to Nuclear Reactor Theory. Addison Wesley Publishing Company.

Lamkin, D.E., 2017. Analytical stress analysis solution for simplified model of a reactor fuel element. PhD. Thesis report, June 2017.

Lassman, K., Hohlefeld, F., 1987. The revised URGAP model to describe the gap conductance between fuel and cladding. Nuclear Engineering and Design 103, 215–221.

Laurent, M., Vuillermoz, P.-L., 1993. Conductivite thermique des solides. Techniques de l'ingenieur. Constantes physico-chimiques 3 (K420). K420–1.

Lecerf, J., Garnier, Y., Girard, J.-M., Domergue, C., Gaubert, L., Manenc, C., 2017. Study of the linearity of CABRI experimental chambers during RIA transients. In: Proc. Int. Conf. ANIMMA2017, Liege, June 2017.

Masoneilan, 1998. Masoneilan Control Valve Sizing Handbook, volume Bulletin OZ1000.

Pascal, V., Alpy, N., Ammar, K., Anderhuber, M., Baudron, A.M., et al., 2020. Multiphysics modelisation of an unprotected loss of flow transient in sodium cooled fast reactors using a neutronic/thermohydraulic coupling scheme. In: Proceedings of PHYSOR 2020, volume 65, cadarache, June 2020.

Ritter, G., Berre, R., Pantera, L., 2012. DULCINEE. Beyond neutron kinetics, a powerful analysis software. In: RRFM IGORR, 2012. Prague, Czech Republic, March 18–22.

Rondeaux, A., 2011. Caractérisation de la puissance déposée dans les barres transitoires du système d'injection de réactivité CABRI. Technological research report, INPG/CEA, Cadarache, April 2011.

Salah, A.-B., Lo Nigro, A., D'Auria, F., et al., 2003. Overview of coupled 3D system thermal-hydraulics neutron kinetics code applications, IAEA-TECDOC-1539. IAEA-TECDOC-1539, IAEA, USA.

Santamarina, A., Bernard, D., Blaise, P., Coste, M., et al., 2009. The JEFF-3.1. 1 nuclear data library. JEFF report, 22(10.2), 2.

Seiler-Marie, N., Marrel, A., Herbreteau, K., 2019. Statistical methodology for a quantified validation of sodium fast reactor simulation tools. Journal of Verification, Validation and Uncertainty Quantification 4, 10.

Su, G.-Y., Bucci, M., McKrell, T., Buongiorno, J., 2016a. Transient boiling of water under exponentially escalating heat inputs. Part I: Pool boiling. International Journal of Heat and Mass Transfer 96, 667–684.

Su, G.-Y., Bucci, M., McKrell, T., Buongiorno, J., 2016b. Transient boiling of water under exponentially escalating heat inputs. Part II: Flow boiling. International Journal of Heat and Mass Transfer 96, 685–698.

Visentini, R., Colin, C., Ruyer, P., 2014. Experimental investigation of heat transfer in transient boiling. Experimental Thermal and Fluid Science 55, 95–105.

Wilson, G.E., Boyack, B.E., 1998. The role of PIRT in experiments, code development and code applications associated with reactor safety assessment. Nuclear Engineering and Design 186, 23–37.